JOURNAL OF GEOPHYSICAL RESEARCH, VOL. 112, D06209, doi:10.1029/2006JD007677, 2007

Oxidation of oleic acid at air/liquid interfaces

Laura F. Voss,[1] Mohamad F. Bazerbashi,[1] Christopher P. Beekman,[1] Christopher M. Hadad,[1] and Heather C. Allen[1]

Received 21 June 2006; revised 22 September 2006; accepted 5 December 2006; published 24 March 2007.

[1] Oxidation of oleic acid monolayers by ozone was studied to understand the fate of fat-coated aerosols from both freshwater and saltwater sources. Oleic acid monolayers at the air/water interface and at the air/sodium chloride solution interface were investigated using surface-specific, broad-bandwidth, sum frequency generation spectroscopy. Complementary techniques of infrared reflection adsorption spectroscopy and surface pressure measurements taken during monolayer oxidation confirmed the sum frequency results. Using this nonlinear optical technique coupled with a Langmuir trough, concurrent spectroscopic and thermodynamic data were collected to obtain a molecular picture of the monolayers. No substantial difference was observed between oxidation of monolayers spread on water and on 0.6 M sodium chloride solutions. Results indicate that depending on the size of the aerosol and the extent of oxidation, the subsequent oxidation products may not remain at the surface of these films, but instead be dissolved in the aqueous subphase of the aerosol particle. Results also indicate that oxidation of oleic acid could produce monolayers containing species that have no oxidized acyl chains.

Citation: Voss, L. F., M. F. Bazerbashi, C. P. Beekman, C. M. Hadad, and H. C. Allen (2007), Oxidation of oleic acid at air/liquid interfaces, *J. Geophys. Res.*, *112*, D06209, doi:10.1029/2006JD007677.

1. Introduction

[2] The possibility that seawater aerosols injected into the atmosphere through mechanical processes may possess a hydrophobic organic monolayer was first proposed by *Gill et al.* [1983] and furthered by *Ellison et al.* [1999]. The resulting aerosol is described as an inverse micelle with the polar carboxylic head groups of the fatty acid (lipid, RCO_2H) oriented into the water droplet and the acyl chains oriented out toward the atmosphere. It is highly likely that similar fat-coated aerosols originate from freshwater sources as well. Since the solubility of surfactants in salt water should be lower than that in freshwater, one might hypothesize that fat coats on sea-salt versus freshwater aerosols may differ in the orientation of the surface fatty acid molecules, thereby potentially affecting rates of reaction between fatty acids and atmospheric oxidants. The role that these fat-coated aerosols play in atmospheric chemistry depends on the oxidation of the hydrophobic shell.

[3] Aerosol growth through uptake of water and volatile organic compounds will only occur when oxidized acyl chains are present in the fat coat [*Ellison et al.*, 1999]. Fieldwork by *Tervahattu et al.* [2002a, 2002b, 2005] demonstrated that fat coats do exist on some marine and continental aerosols and that oleic acid [$CH_3(CH_2)_7CH{=}CH(CH_2)_7CO_2H$] is the most prevalent unsaturated fatty acid found in the fat coats of marine aerosols. Furthermore, the measurements showed no indication of oxidized acyl chains on the surface of the aerosols, despite atmospheric lifetimes that are long enough to react with common oxidants. The authors suggested that the oxidation products may either evaporate from the surface or partition into the aqueous subphase.

[4] Oleic acid has emerged as a model system used to study atmospheric oxidation of organic materials due to its prevalence in tropospheric particulate matter [*Rogge et al.*, 1991]. Studies have focused on heterogeneous reactions of liquid oleic acid in coated flow tubes [*Moise and Rudich*, 2002; *Thornberry and Abbatt*, 2004], as aerosols [*Katrib et al.*, 2004; *Morris et al.*, 2002; *Smith et al.*, 2003], and most recently as millimeter-sized droplets [*Hung et al.*, 2005]. Few studies have focused on the oxidation of monolayers at the air/water interface [*Eliason et al.*, 2004; *Mmereki et al.*, 2004; *Raja and Valsaraj*, 2005; *Srisankar and Patterson*, 1979; *Voss et al.*, 2006; *Wadia et al.*, 2000]. Of these, *Srisankar and Patterson* [1979], *Voss et al.* [2006], and *Wadia et al.* [2000] studied oxidation of oleic acid chains at the air/water interface, with the latter being a study of 1-oleoyl-2-palmitoyl-*sn*-glycero-3-phosphocholine, a phospholipid with a $CH_3(CH_2)_7CH{=}CH(CH_2)_7$ chain identical to the acyl chain on oleic acid. In their work, *Srisankar and Patterson* [1979] reported monolayer disruption with the introduction of ozone by measuring the decrease in surface pressure. *Voss et al.* [2006] recently reported a secondary effect of oleic acid oxidation by studying the replacement of the ozone oxidation products with less-soluble species from the aqueous subphase for mixed monolayer systems. *Wadia et al.* [2000] reported the formation of gas-phase oxidation products in real time using

[1]Department of Chemistry, The Ohio State University, Columbus, Ohio, USA.

0148-0227/07/2006JD007677$09.00

atmospheric pressure ionization mass spectrometry. In this paper, we report results of experiments designed to probe the molecular properties of oleic acid monolayers at the air/water interface and the air/sodium chloride solution interface, to study the ozone-mediated oxidation of the monolayer, and to evaluate the subsequent fate of the oxidized products.

[5] Sum frequency generation (SFG) vibrational spectroscopy provides a tool to study monolayer systems at the air/water interface, as presented in a pioneering work by Y. R. Shen and coworkers [*Guyot-Sionnest et al.*, 1987] and the Eisenthal group [*Vogel et al.*, 1991]. Our broad-bandwidth, sum frequency generation (BBSFG) spectroscopy experiment simultaneously probes spectral regions as large as 500 cm^{-1} in width by overlapping a picosecond 800-nm pulse with a spectrally broad femtosecond infrared pulse in space and time on the sample surface [*Hommel et al.*, 2001; *Ma and Allen*, 2003]. As the theory of SFG has been treated extensively in the literature [*Gopalakrishnan et al.*, 2006; *Hirose et al.*, 1992; *Miranda and Shen*, 1999; *Richmond*, 2002; *Zhang et al.*, 1994], only a summary of the details necessary for understanding this work is discussed here. The generation of signal from the anti-Stokes Raman scattering from an infrared excited surface requires that selection rules for both spectroscopic methods be met, which leads to a requirement for a lack of inversion symmetry. The breaking of symmetry at the interface provides this lack of inversion. The signal intensity from this surface-specific technique depends not only on number density but also on the orientation of molecules present at the interface. This broad-bandwidth technique allows for a vibrational spectrum to be obtained from each laser pulse, minimizing data acquisition time and, in doing so, providing better signal-to-noise ratios than most scanning SFG systems. The rapid acquisition of spectra from the monolayer at the air/water interface allows monitoring of dynamic processes, such as the ozone-mediated oxidation of an oleic acid monolayer. SFG spectroscopy has been used to study lipid monolayers at the air/water interface in model biological systems, as recently reviewed by *Chen et al.* [2005]. Furthermore, we use complementary experimental techniques to confirm our SFG results. Herein, we present an SFG study of oleic acid monolayers at air/liquid interfaces developed to understand atmospheric processes.

2. Experimental Method

[6] The BBSFG experimental setup, described elsewhere [*Hommel et al.*, 2001; *Ma and Allen*, 2003], is detailed briefly here. A single titanium:sapphire laser (Spectra Physics Tsunami) seeds and a single neodymium:yttrium lithium fluoride laser (Spectra Physics Evolution) pumps two 1-kHz regenerative amplifiers (Spectra Physics Spitfire) designed to generate 2-ps pulses and 85-fs pulses. The femtosecond beam is used in an optical parametric amplifier with a difference frequency generation crystal (Spectra Physics OPA-800F) to produce tunable infrared light with a broad spectral bandwidth. In this study, the optical parametric amplifier was tuned so that the infrared light was centered at 2900 cm^{-1} to cover the C–H stretching region of the acyl chain of oleic acid and had a spectral bandwidth of $\sim$300 cm^{-1}. Using turning and focusing optics, the infrared beam and the picosecond 800-nm beam are overlapped spatially at the sample surface. Adjusting a retroreflector on a micrometer stage in the 800-nm beam line allows the beams to be overlapped temporally as well. The input energy to the sample surface of the 800-nm beam was 250 μJ/pulse. The infrared input energy to the sample surface was 8 μJ/pulse. The resulting SFG signal is detected in reflection at the output angle determined by the angle of the input beams and the conservation of momentum. The signal is spectrally dispersed using a monochromator (Acton Research SpectroPro 0.5 m) with the entrance and exit slits fully open and collected using a back-illuminated, liquid-nitrogen-cooled charge-coupled device (Roper Scientific 400 EB). The resolution of 8 cm^{-1} is limited by the bandwidth of the spectrally chirped portion of the visible beam that overlaps in time with the broad-bandwidth infrared beam and is confirmed by comparison to Fourier transform infrared (FT-IR) spectra of variable resolution [*Ma and Allen*, 2006]. Polarization optics for both the input beam lines and the signal detection line are used to select the polarization of these beams. BBSFG data reported in this work were recorded in the SSP polarization combination for the SFG signal, the 800-nm beam, and the infrared beam, respectively. SPS and PPP polarization combination data were also obtained for oleic acid monolayers at the air/water interface and are included in the supplemental material. The spectra were background-subtracted and normalized to the nonresonant SFG signal produced from a GaAs crystal and were calibrated to the 2848.5-cm^{-1} absorption of polystyrene.

[7] Oleic acid (99%, Sigma Aldrich, CAS 112-80-1) and oleic acid–ozone reaction products, nonanoic acid (96%, Aldrich, CAS 112-05-0), azelaic acid (98%, Aldrich, CAS 123-99-9), and nonanal (95%, Aldrich, CAS 124-19-6), were used as received without further purification. Solutions of each were prepared in chloroform (99.8%, Sigma Aldrich, CAS 67-66-3). Monolayers were spread on deionized water with a resistivity of 18.3 MΩ cm (Barnstead Nanopure). All experiments were conducted at room temperature (23°C) and at atmospheric pressure.

[8] Surface pressure–area isotherms were performed with a low-volume Langmuir trough (KSV Instruments Limited Minitrough) equipped with two Delrin barriers used to symmetrically compress the film. The surface pressure was monitored during film compression using a platinum Wilhelmy plate. The aqueous subphase was replaced after each experiment. A measured volume of oleic acid solution was spread on deionized water with the barriers in the open position using a 50-μL Hamilton syringe. Ten minutes elapsed before isothermal compression to allow the chloroform solvent to evaporate. The barriers were compressed at a rate of 5 mm/min. BBSFG spectra were taken currently with isotherm compression data.

[9] For BBSFG oxidation experiments, monolayers of oleic acid were spread on 20 mL of deionized water in a Pyrex petri dish that was placed in a Teflon cell equipped with windows to pass the incoming and outgoing beams. A 50-μL Hamilton syringe was used to spread the lipid solution on the water surface. The quantity of oleic acid spread was equivalent to 32 $Å^2$/molecule, resulting in a monolayer of the condensed phase as reported previously [*Goncalves da Silva and Romao*, 2005] and confirmed in this work. Ten minutes elapsed before BBSFG data acqui-

sition began so as to allow the chloroform solvent to evaporate completely.

[10] Ozone for the BBSFG experiments was generated by flowing O_2 (99.997%, Praxair) through a pen-ray lamp ozone generator (Jelight model 600). The concentration of ozone is calculated by measuring the absorbance at 254 nm (Ocean Optics USB 2000 spectrometer) and applying Beer's law using the molar absorption coefficient of 1.15×10^{-17} cm^2/molecule [*Finlayson-Pitts and Pitts*, 2000] for the 10-cm path length. The O_2 flow was controlled using a mass flow controller (MKS Instruments, 1479A51CS1BM). A second mass flow controller allowed the introduction of N_2 (99.999%, Praxair) into the ozone stream to dilute the ozone concentration. The ozone concentration for the BBSFG experiments was approximately 20 ppm with a flow rate of 15 standard cubic centimeters per minute (sccm). Using identical experimental conditions resulted in reproducible trends reported below. The data in this work represent six individual experiments.

[11] Oleic acid monolayer oxidation experiments were also conducted on sodium chloride solutions. Solutions were prepared to replicate the ~0.6 M salt concentration found in seawater [*Howe*, 1974]. Sodium chloride (certified ACS, Fisher Scientific, CAS 7647-14-5) was dissolved in deionized water. The resulting solution was filtered through a Whatman Carbon-Cap activated carbon filter to remove organic contaminants. The concentration of the filtered solution was determined by the Mohr titration technique [*Finlayson*, 1992] using silver nitrate (reagent grade, Fisher Scientific, CAS 7761-88-8) and potassium chromate (99.5%, E.M. Science, CAS 7789-00-6). This stock solution was then diluted in deionized water to a final concentration of 0.6 M. Oleic acid was spread on the sodium chloride solutions at equilibrium spreading pressure to result in monolayers with a mean molecular area of 32 $Å^2$/molecule.

[12] Monolayers of the oleic acid–ozone oxidation products, nonanoic acid, azelaic acid, and nonanal, were prepared in the same manner as the oleic acid monolayer. For these species, however, data acquisition began immediately after spreading to take into account that they may have dissolved into the subphase before 10 min elapsed.

[13] In addition to the BBSFG experiments, complementary infrared reflection absorption spectroscopy (IRRAS) experiments of monolayer oxidation were also performed. IRRAS spectra were obtained using a Thermo Nicolet spectrometer (Avatar 370, Thermo Electron Corporation). Monolayers with a mean molecular area of 32 $Å^2$/molecule of oleic acid were spread at the air/water interface in a rectangular Teflon dish containing 50 mL of deionized water. Two 2-in. diameter gold mirrors were positioned 4 in. apart on a breadboard in the FT-IR chamber to direct the unpolarized IR beam to and from the air/water interface with a 35° angle of incidence with respect to the sample surface. A micrometer-controlled sample stage was used to adjust the height of the sample. Spectra were collected at a resolution of 4 cm^{-1} and averaged over 500 scans.

[14] For the IRRAS and Langmuir trough oxidation experiments, ozone was generated using a Sharper Image Ionic Breeze Personal Air Purifier (model # SI7362TN), a device that has been proven to generate ozone [*Britigan et al.*, 2006]. The concentration of ozone inside the sample chamber of the FT-IR spectrometer was monitored during ozonolysis of the monolayer by bubbling samples of the purge gas through a 0.06 M potassium iodide (CAS 7681-11-0) solution buffered with 0.1 M boric acid (CAS 10043-35-3) [*Seeley et al.*, 2005]. The concentration of the resultant tri-iodide oxidation product was determined by measuring the absorption at 352 nm using the Ocean Optics USB-2000 spectrometer and applying Beer's law using the molar absorptivity of 27,636 M^{-1} cm^{-1} [*Mamane et al.*, 2006]. Ozone concentrations were calculated using the flow rate of gas exiting the FT-IR spectrometer (460 mL/min) and the relationship:

$$O_3(g) + 3I^-(aq) + 2H^+(aq) \rightarrow I_3^-(aq) + O_2(g) + H_2O.$$

Ozone concentrations averaged 190 ± 80 ppb by volume during ozonolysis of the oleic acid monolayer. This method was also used to generate ozone to monitor the surface pressure of oleic acid monolayers in the Langmuir trough during oxidation.

3. Results and Discussion

[15] Before discussing the oxidation of oleic acid by ozone, we first present a brief study of oleic acid monolayers at the air/water interface. In Figure 1, isothermal compression data taken with the Langmuir trough is presented with BBSFG spectra taken during the compression. Accumulation time for each spectrum was 30 s. There are three distinct regions in the pressure–area isotherm: the liquid–gas coexistence region above the phase transition at 51 $Å^2$/molecule, the liquid phase region from 28 to 51 $Å^2$/molecule, and the film-collapse region below 28 $Å^2$/molecule. The isotherm is representative of typical oleic acid isotherms [*Gaines*, 1966; *Goncalves da Silva and Romao*, 2005]. The BBSFG spectra represent these distinct regions. Figure 1a is the spectrum taken just before isothermal compression begins. The spectra taken from the beginning of compression until the phase transition were identical to this spectrum. Figure 1b is the spectrum taken just after the phase transition. As the compression continued, the spectra evolved with increasing peak heights until Figure 1c was obtained, just prior to the film's collapse. The spectra taken after the film's collapse were essentially identical to Figure 1c.

[16] Figure 2 is a 2-min spectrum of an oleic acid monolayer spread on deionized water at equilibrium-spreading pressure in a petri dish with a mean molecular area of 32 $Å^2$/molecule. This spectrum is qualitatively similar to the one in Figure 1c. The peaks present in the oleic acid spectra are the CH_2 symmetric stretch (2846 cm^{-1}), the CH_3 symmetric stretch (2876 cm^{-1}), the CH_2 Fermi resonance (2923 cm^{-1}), the CH_3 Fermi resonance (2941 cm^{-1}), and the =CH olefinic stretch at the carbon–carbon double bond (3014 cm^{-1}), following assignments and arguments made by *Lu et al.* [2005] and commonly known infrared and Raman vibrational assignments [*Socrates*, 2001].

[17] The concurrent pressure–area isotherm data and BBSFG data provide a picture of the oleic acid monolayer at a molecular level. Before the phase transition, the oleic acid molecules were dispersed and disordered. This is evident in the BBSFG data by the absence of the oleic acid C–H stretching peaks. While the oleic acid was present at the air/water interface, the few, disordered molecules probed

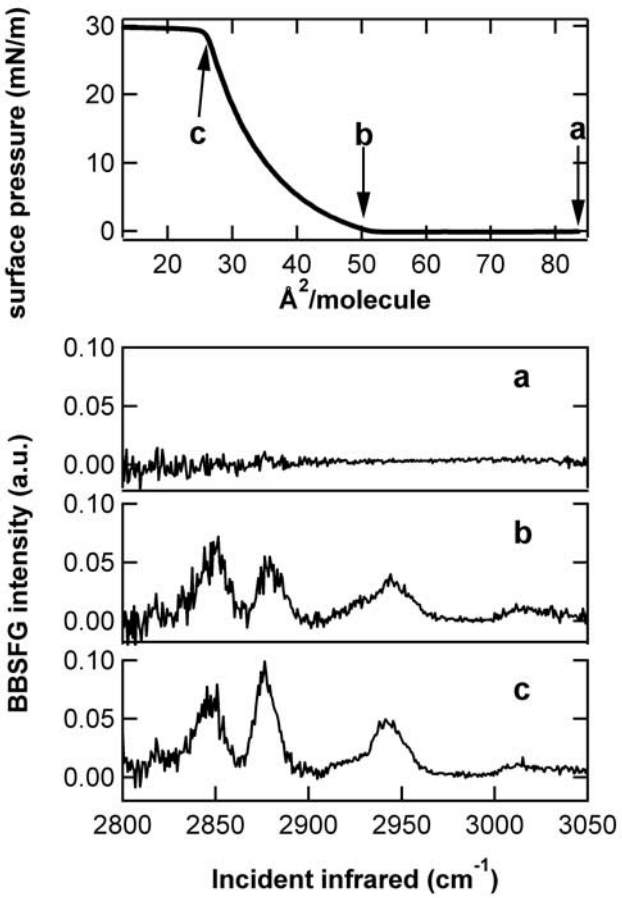

Figure 1. Concurrent Langmuir compression isotherm data and BBSFG spectra of an oleic acid monolayer at the air/water interface. Top graph is the Langmuir isotherm with markers indicating where BBSFG spectra are taken (a) before beginning compression at 83 Å^2/molecule, (b) just after the first-order phase transition evident at 51 Å^2/molecule, and (c) just before the film collapses at 28 Å^2/molecule.

by the overlapping laser beams were below the detection limit of the BBSFG experiment. The thermodynamic data indicate that the monolayer underwent a phase transition from the liquid–gas coexistence region to the liquid phase at 51 Å^2/molecule. This is evident in the BBSFG data, with oleic acid peaks appearing in the spectra immediately after this phase transition. As the compression continued, the monolayer became more ordered until the film collapsed when the applied pressure exceeded the oleic acid equilibrium spreading pressure of 30 mN/m [*Gaines*, 1966]. After this point, the monolayer was in equilibrium with miniscule droplets of condensed oleic acid. The BBSFG data support the observations of the pressure–area isotherm as the C–H peaks of the oleic acid continued to intensify as compression of the liquid phase ordered the monolayer. After monolayer collapse, equilibrium between the monolayer and the droplets maintained the monolayer order.

[18] The changes in the ratio of the peak intensity of the CH_3 symmetric stretch relative to the CH_2 symmetric stretch are evident in Figures 1b and 1c. In the more ordered film, just before film collapse, the CH_3 symmetric stretch is more predominant than the CH_2 symmetric stretch. The opposite is true in the less-ordered film, just after the phase transition. In the oleic acid monolayer spread at equilibrium spreading pressure (Figure 2), the CH_3 symmetric stretch peak is the most intense peak in the spectrum, indicating that the oleic acid was in a well-ordered state at the mean molecular area of 32 Å^2/molecule.

[19] The oleic acid oxidation experiments were conducted in a closed cell. Spatial limitations make enclosing the Langmuir trough with the BBSFG sample stage awkward and complicated. To overcome this complication, we spread oleic acid on 20 mL of deionized water in a 5-cm diameter Pyrex petri dish to achieve a mean molecular area of 32 Å^2/molecule and used an experimental cell designed to hold the petri dish and contain the ozone until it was vented to the exhaust. Both Figures 2 and 3a are the BBSFG spectra of such oleic acid monolayers. The differences between these spectra are simply the effects of having the lid off (Figure 2) and on the cell (Figure 3a) and of decreasing the data collection time from 2 min to 30 s, respectively.

[20] Thus, Figure 3a is the 30-s spectrum of an oleic acid monolayer, and the data were accumulated just before the introduction of ozone. Ozone, at a concentration of 20 ppm, flowed over the surface and out of the cell, whereas BBSFG spectra were acquired over 30-s accumulations. Figure 3b is the spectrum taken after 1 min of ozone exposure. The most significant difference between this spectrum and Figure 3a is the decrease in the peak intensity of the CH_3 symmetric stretch. Figure 3c is the spectrum taken after 2 min of ozone exposure. In this spectrum, the CH_3 symmetric stretching peak is hardly visible. Figures 3d and 3e are the spectra taken after 10 and 30 min of ozone exposure, respectively. These spectra show that after continued ozone exposure, the

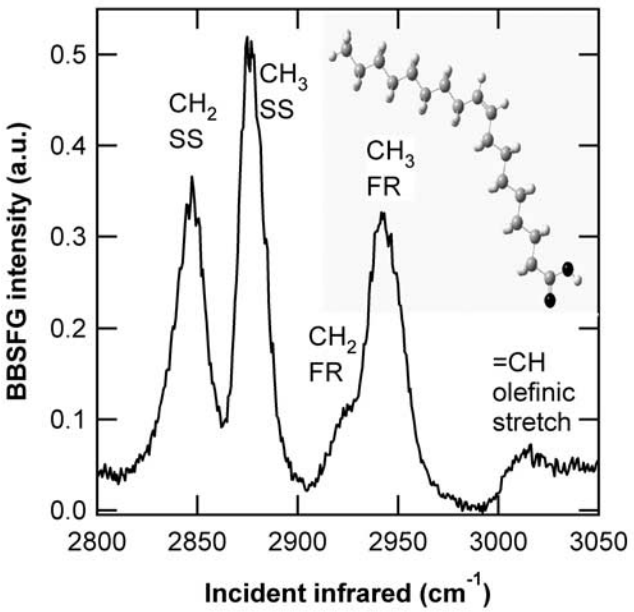

Figure 2. BBSFG spectrum of an oleic acid monolayer on water at a surface coverage of 32 Å^2/molecule. Peaks are the CH_2 symmetric stretch (2846 cm^{-1}), the CH_3 symmetric stretch (2876 cm^{-1}), the CH_2 Fermi resonance (2923 cm^{-1}), the CH_3 Fermi resonance (2941 cm^{-1}), and the sp^2 olefinic =CH stretch (3014 cm^{-1}).

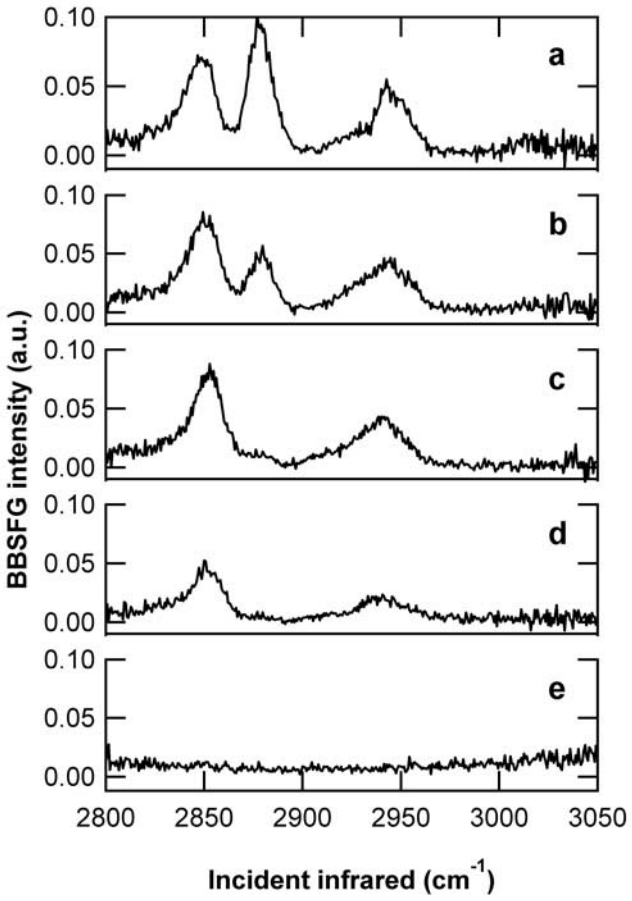

Figure 3. Oxidation of oleic acid monolayer at the air/water interface with ozone. A 32 Å^2/molecule monolayer of oleic acid forms at equilibrium spreading pressure. BBSFG spectra are taken (a) before exposure to ozone and (b) after 1-min exposure, (c) after 2-min exposure, (d) after 10-min exposure, and (e) after 30-min exposure.

peaks continued to decrease in intensity until there was no spectroscopic evidence of oleic acid at the air/water interface. This is confirmed by removing the cell lid and taking 2-min spectra at the end of the experiment. We conclude therefore that the oxidized oleic acid is removed from the interfacial surface, and the oxidized products are distributed in the aqueous subphase and in the gas phase.

[21] In our SFG experiments, a random orientation of oleic acid and its reaction products would create a macroscopic inversion center and therefore SFG inactivity. To investigate this aspect further, complementary IRRAS experiments at the air/water interface were conducted. Monolayers were spread at the air/water interface, and then ozone was generated using the Shaper Image air purifier at a concentration of ~190 ppb. Spectrum (a) of Figure 4 shows the monolayer before the introduction of ozone. The peaks are the CH_2 symmetric stretch (2854 cm^{-1}) and the CH_2 asymmetric stretch (2923 cm^{-1}). The subsequent spectra (b–f) are 10-min spectra taken during oxidation. Unlike the interface-specific SFG experiment, a volume of solution is evaluated at the air/water interface in the IRRAS experiment. After oxidation by ozone, the resulting IRRAS spectra confirm that all C–H stretches are absent from the probe volume and that neither oleic acid nor its reaction products are observed. Similar to the SFG experiments, the spectral intensity of the CH_2 stretching peaks decreases with oxidation time until these peaks are no longer observable in the IRRAS spectra.

[22] The removal of organic material from the air/water interface through oxidation of oleic acid by ozone is further confirmed by oxidizing monolayers while monitoring the change in surface pressure. Using the Langmuir trough and deionized water, the balance attached to the Wilhelmy plate was zeroed to the value of the surface pressure of water. Oleic acid was then spread at the air/water interface. The monolayer was compressed to a surface pressure of 30.5 mN/m. The film was allowed to equilibrate for 2.5 min before the personal air purifier was turned on to generate ozone at ~190 ppb. Figure 5 shows the change in surface pressure during oxidation. The drop in surface pressure to the zeroed value of the surface pressure of water is further indication that the organic material is no longer present at the air/water interface.

[23] The results of experiments on pure water provide information about processes that may occur on aerosols from freshwater sources. The aqueous cores of the marine aerosols will be composed of solutions reflecting the composition of the sea from which they originated. Seawater has a salt concentration of ~0.6 M and is a complex ionic mixture [*Howe*, 1974]. We prepared solutions of 0.6 M sodium chloride as a first approximation to replicate seawater solutions and spread oleic acid at equilibrium spreading pressure on these solutions to produce a monolayer with

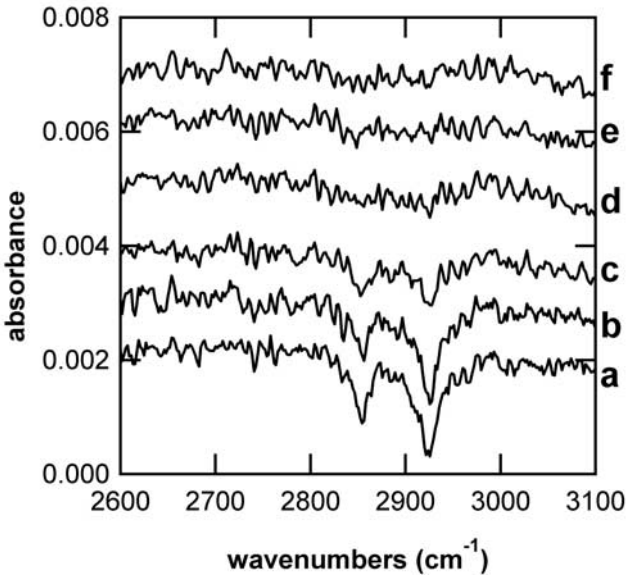

Figure 4. IRRAS spectra of oleic acid monolayer on deionized water during oxidation. Oleic acid was spread at equilibrium spreading pressure to result in a monolayer with a mean molecular area of 32 Å^2/molecule. Peaks are the CH_2 symmetric stretch (2854 cm^{-1}) and the CH_2 asymmetric stretch (2923 cm^{-1}). Ozone at ~190 ppb was generated with a personal air purifier and allowed to react with the monolayer. Spectra are offset for clarity and represent (a) before the introduction of ozone and (b)–(f) 10-min intervals after the start of ozone exposure.

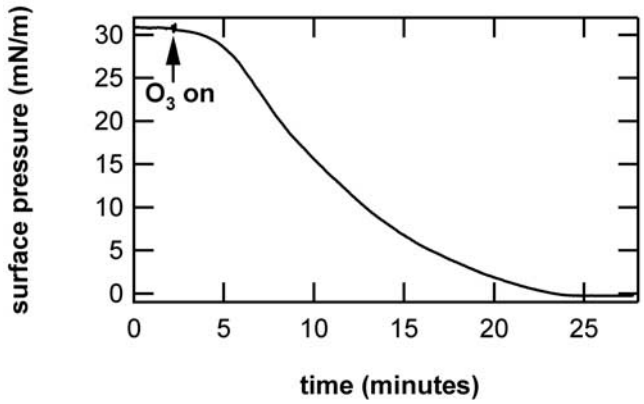

Figure 5. Surface pressure of oleic acid monolayer during oxidation. Using deionized water in the Langmuir trough, the balance was zeroed so that the surface pressure due to water would be zero. Oleic acid was spread at the air/water interface and then compressed to a surface pressure of 30.5 mN/m. The film was allowed to equilibrate for 2.5 min before the ozone generator was turned on.

a mean molecular area of 32 Å^2/molecule. Figure 6 is the BBSFG spectrum of an oleic acid monolayer on a 0.6 M sodium chloride solution taken with a 2-min accumulation time. This spectrum is qualitatively similar to the spectrum of the equivalent oleic acid monolayer spread on water presented in Figure 2. There is, however, a different intensity ratio between the CH_3 and the CH_2 symmetric stretch peaks in the monolayers spread on water versus the sodium chloride solution. This indicates that the molecular orientation and/or conformation at the air/water interface is somewhat different between the two systems. Further comment on the extent of these differences would be purely speculative. The differences, however, do not seem to affect the oxidation of the monolayer. Results of oxidation of this monolayer with 20-ppm ozone are presented in Figure 7. The spectra are derived from 30-s accumulations. These results show the same trend as the results of the oxidation of the oleic acid monolayer at the air/water interface presented in Figure 3, with the first change being in the height of the CH_3 symmetric stretch peak and then the subsequent disappearance of all C–H stretching peaks from the spectra. This result also implies that the reaction rates of oleic acid at the surface of a seawater versus a freshwater aerosol are similar.

[24] Since by the end of the oxidation experiments there was no evidence of organic material present at the air/liquid interface, one question that begs answering is what was the organic material present in the monolayer after only a few moments of ozone exposure. From the BBSFG data, the spectra clearly change. Could these spectra be ozone oxidation products of oleic acid that may be present at the interface? To answer this question, monolayer equivalents

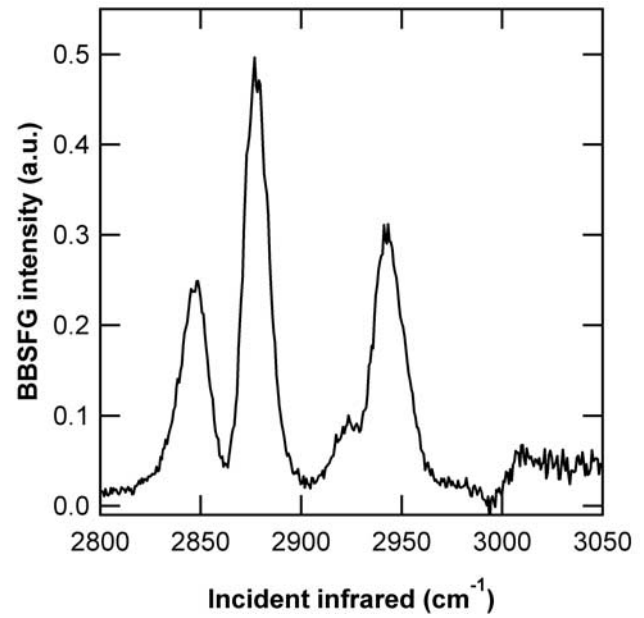

Figure 6. BBSFG spectrum of oleic acid monolayer on 0.6 M sodium chloride solution. Oleic acid was spread at equilibrium spreading pressure to result in a monolayer with a mean molecular area of 32 Å^2/molecule.

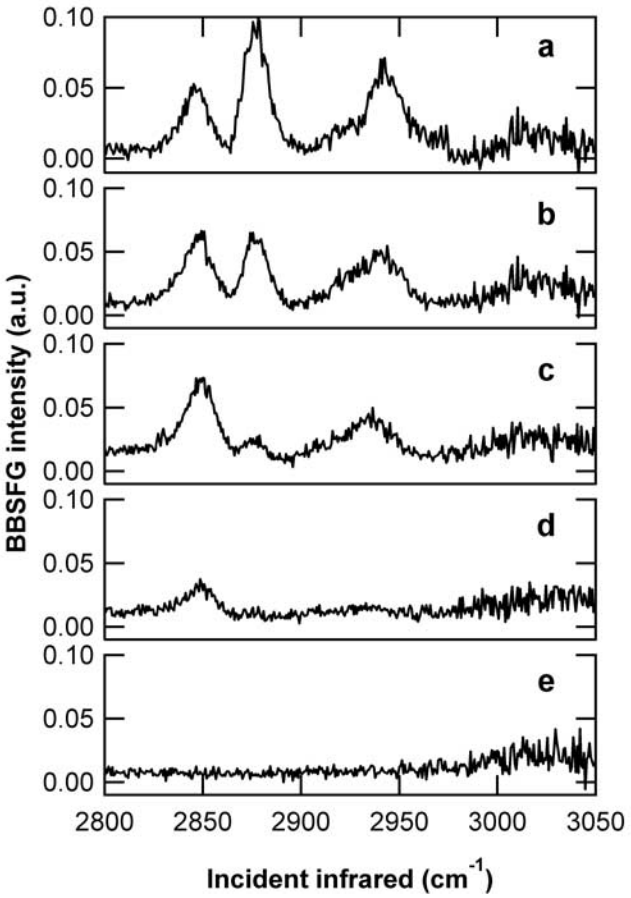

Figure 7. Oxidation of oleic acid monolayer on a sodium chloride solution with ozone. A 32 Å^2/molecule monolayer of oleic acid forms at equilibrium spreading pressure at the air/sodium chloride solution interface. Just as in the oxidation experiment at the air/water interface presented in the data of Figure 3, BBSFG spectra are taken (a) before exposure to ozone and (b) after 1-min exposure, (c) after 2-min exposure, (d) after 10-min exposure, and (e) after 30-min exposure.

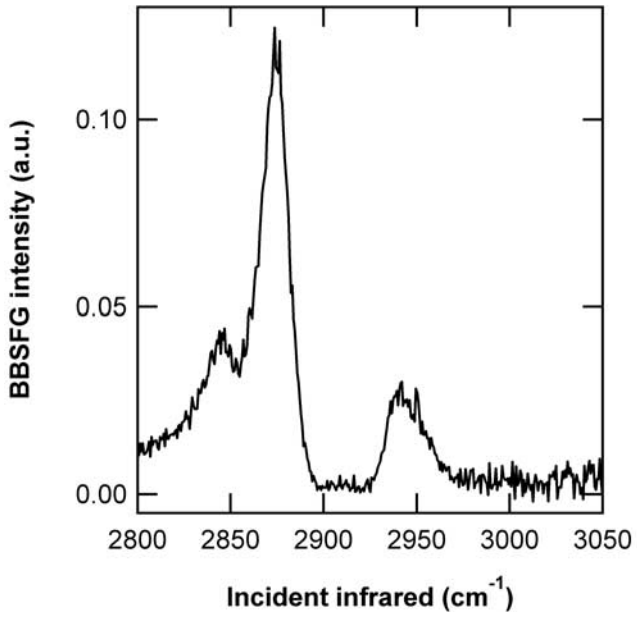

Figure 8. BBSFG spectra of three-monolayer equivalents of nonanal at the air/water interface.

of the final reaction products were spread at the air/water interface. In the gas phase, ozone reacts with oleic acid at the C=C bond to ultimately produce nonanal [$CH_3(CH_2)_7CHO$], nonanoic acid [$CH_3(CH_2)_7CO_2H$], azelaic acid [$HO_2C(CH_2)_7CO_2H$], and 9-oxononanoic acid [$OCH(CH_2)_7CO_2H$; *Moise and Rudich*, 2002]. The solubilities of these species are (in g/L) 9.6×10^{-2}, 2.8×10^{-1}, 2.4 [*Yalkowsky and He*, 2003], and 19, respectively [*King*, 1938]. Not surprisingly, there was no spectroscopic evidence of nonanoic acid or azelaic acid when five monolayer equivalents of each were spread at the air/water interface. The high solubility of these products in the aqueous subphase guaranteed that these species are not present at the interface in concentrations high enough to be detected in the 50 μM solutions that result. Given that 9-oxononanoic acid is even more soluble than these species, similar results are expected for that product (although testing was not performed due to the high cost of the material). Similar results were obtained with two monolayer equivalents of nonanal. When a third monolayer equivalent was spread, however, the C–H stretching peaks of nonanal were evident in the BBSFG spectrum, as shown in Figure 8.

[25] Comparison of the spectral results of three monolayer equivalents of nonanal at the air/water interface with the oleic acid–ozone oxidation indicates that the initial changes in the spectra were not due to the presence of nonanal at the air/water interface. In the spectrum of nonanal at the air/water interface presented in Figure 8, the peak from the CH_3 symmetric stretch is the most intense. For comparison, the spectra taken after 1 and 2 min of ozone exposure presented as Figures 3b and 3c show a CH_3 symmetric stretch peak that is lower in intensity than the CH_2 symmetric stretch. Furthermore, nonanal is volatile at room temperature and can be detected by gas-phase analysis after oxidation of oleic acid [*Wadia et al.*, 2000]. Therefore it is most likely that the nonanal produced from the oxidation reaction is removed from the cell by the gas flow.

[26] Polymerization of alkenes during the reaction with ozone has been observed in previous experiments on condensed phase fatty acid droplets [*Hung et al.*, 2005] and tethered monolayers [*McIntire et al.*, 2005]. We cannot confirm polymerization at the air/water interface in our studies using BBSFG or IRRAS. These experiments coupled with the surface pressure experiments indicate that there is no organic material remaining at the air/water interface after oxidation. This indicates that if polymerization is occurring, then the oxidized species are being solubilized in the subphase and are therefore not present at the air/water interface. It may also be possible that the reaction of ozone with unsaturated species from a pure condensed phase oleic acid droplet or alkene chains tethered to a solid substrate has an alternative reaction pathway to an oleic acid monolayer on an aqueous subphase, as studied here.

[27] Having ruled out the likelihood that the spectral changes were from the presence of oxidation products at the air/water interface, we revisit the results of the isothermal compression data to understand the results from the oleic acid oxidation. Again, Figure 1b is the spectrum of the monolayer in a less-ordered liquid state than the fully compressed monolayer. The similarities between this spectrum and the one of the oleic acid monolayer after a minute of ozone exposure (Figure 3b) are striking. Both show similar peak intensity ratios between the CH_3 symmetric stretch and the CH_2 symmetric stretch, with the CH_3 stretch being less intense than the CH_2 stretch. The data indicate that the spectra presented in Figures 3b–3d are of a disordered oleic acid monolayer.

4. Atmospheric Implications

[28] Our results provide insight into the oxidation of tropospheric aerosols by studying a monolayer of oleic acid on the surface of 20 mL of water as a proxy for an atmospheric aerosol. Consider a 0.2-μm diameter spherical water aerosol particle with a pure oleic acid monolayer coating the surface with a mean molecular area of 32 $Å^2$/molecule: the volume of the water core is 4×10^{-18} L, the surface area is 1.3×10^{-13} m^2, and the total number of oleic acid molecules on the surface is 4×10^5. When the oleic acid monolayer is completely oxidized by ozone, there are 6×10^5 molecules of reaction products associated with the water core, assuming nonanal evaporates. Given the solubility of the possible remaining reaction products, the volume of water cannot solvate all of the molecules, and therefore organic material would remain on the surface. The volume of water present in the aerosol could, however, solvate up to 20% of the reaction products. It follows that if less than 20% of the oleic acid monolayer is oxidized, then the reaction products may all be solvated in the water core and not be present on the surface, as is observed in the analysis of fat coats of marine aerosols [*Tervahattu et al.*, 2002a, 2002b].

[29] Simple geometry proves that the volume of the aerosol increases more than the surface area by a factor of one third of the radius as the radius increases. Therefore as the size of the aerosol increases, the volume of the water core increases more than the number of oleic acid molecules present on the surface. Following this logic, aerosols with diameters greater than 1.2 μm have water core volumes great enough to solvate 100% of the oxidation products by

ozone with oleic acid. Note that *Ellison et al.* [1999] predicted fat-coated marine aerosols with diameters of 0.1–5 μm, and *Tervahattu et al.* [2002a, 2002b] measured atmospheric aerosol particles within this range.

5. Conclusions

[30] The studies presented in this work support the conclusions of *Tervahattu et al.* [2002a, 2002b] that fatty acid coats on marine aerosols could react with tropospheric oxidants and yet have no species with oxidized acyl chains on the surface. The oleic acid–ozone oxidation products can evaporate, in the case of nonanal, and others can dissolve into the aqueous subphase until the water core is saturated. Our previous studies indicated that the least soluble species will remain on the surface and that the more soluble components will partition into the subphase [*Voss et al.*, 2006]. For the nonvolatile products from the reaction of ozone with oleic acid, the least soluble species is nonanoic acid, which would be oriented on the surface with the unoxidized alkyl chain directed into the atmosphere. This reaction product will occupy all available surface sites unless the number of surface sites exceeds the number of nonanoic acid molecules. Since oxidation of oleic acid monolayers on both pure water and 0.6 M sodium chloride solutions produced similar results, this argument can be made for fat-coated aerosols originating from freshwater sources as well as from seawater.

[31] Similar results are expected with the oxidation of hydrocarbons by hydroxyl radical, another major tropospheric oxidant. For example, hydroxyl radical reactions with hexadecane produces hexadecanone, short-chain aldehydes, and short-chain carboxylic acids [*Eliason et al.*, 2004]. Since the starting material on the surface of an atmospheric aerosol is a long-chain fatty acid, the oxidation products with OH radical have two oxidized functional groups and are therefore more soluble in the aqueous subphase of an inverse micelle aerosol than the starting product. The oxidation products of the acyl chains and OH radical, too, can partition into the subphase until it is saturated, again resulting in an atmospheric aerosol with no oxidized acyl chains in the fat coat.

[32] Clearly the oxidation of the oleic acid is disrupting the order of the monolayer. It is plausible that once the monolayer is no longer well ordered, the underlying aqueous subphase could evaporate or fragment. In an aerosol, the water core could evaporate until the surface area matched the area required for a well-ordered monolayer. If such a scenario were to occur, oxidation of the fat coat would actually lead to smaller aerosols that still may not possess oxidized species on the surface.

[33] **Acknowledgments.** We acknowledge the National Science Foundation (ATM-0413893 and CHE-0089147) for funding this work. We also acknowledge S. Gopalakrishnan for conducting preliminary experiments with oleic acid and ozone oxidation. L.F.V. acknowledges support through a Camille and Henry Dreyfus Environmental Chemistry Postdoctoral Fellowship.

References

Britigan, N., A. Alshawa, and S. A. Nizkorodov (2006), Quantification of ozone levels in indoor environments generated by ionization and ozonolysis air purifiers, *J. Air Waste Manage. Assoc.*, *56*, 601–610.

Chen, X., M. L. Clarke, J. Wang, and Z. Chen (2005), Sum frequency generation vibrational spectroscopy studies on molecular conformation and orientation of biological molecules at interfaces, *Int. J. Mod. Phys. B*, *19*(4), 691–713.

Eliason, T. L., J. B. Gilman, and V. Vaida (2004), Oxidation of organic films relevant to atmospheric aerosols, *Atmos. Environ.*, *38*(9), 1367–1378.

Ellison, G. B., A. F. Tuck, and V. Vaida (1999), Atmospheric processing of organic aerosols, *J. Geophys. Res.*, *104*(D9), 11,633–11,641.

Finlayson, A. C. (1992), The pH range of the Mohr titration for chloride ion can be usefully extended to 4–10.5, *J. Chem. Educ.*, *69*(7), 559.

Finlayson-Pitts, B. J., and J. N. Pitts Jr. (2000), *Chemistry of the Upper and Lower Atmosphere*, Elsevier, New York.

Gaines, G. L., Jr. (1966), *Insoluble Monolayers at Liquid–Gas Interfaces*, John Wiley, Hoboken, N. J.

Gill, P. S., T. E. Graedel, and C. J. Weschler (1983), Organic films on atmospheric aerosol particles, fog droplets, cloud droplets, raindrops, and snowflakes, *Rev. Geophys. Space Phys.*, *21*(4), 903–920.

Goncalves da Silva, A. M., and R. I. S. Romao (2005), Mixed monolayers involving DPPC, DODAB and oleic acid and their interaction with nicotinic acid at the air–water interface, *Chem. Phys. Lipids*, *137*(1–2), 62–76.

Gopalakrishnan, S., D. Liu, H. C. Allen, M. Kuo, and M. J. Shultz (2006), Vibrational spectroscopic studies of aqueous interfaces: salts, acids, bases, and nanodrops, *Chem. Rev.*, *106*(4), 1155–1175.

Guyot-Sionnest, P., J. H. Hunt, and Y. R. Shen (1987), Sum-frequency vibrational spectroscopy of a Langmuir film: Study of molecular orientation of a two-dimensional system, *Phys. Rev. Lett.*, *59*(14), 1597–1600.

Hirose, C., N. Akamatsu, and K. Domen (1992), Formulas for the analysis of surface sum-frequency generation spectrum by CH stretching modes of methyl and methylene groups, *J. Chem. Phys.*, *96*(2), 997–1004.

Hommel, E. L., G. Ma, and H. C. Allen (2001), Broadband vibrational sum frequency generation spectroscopy of a liquid surface, *Anal. Lett.*, *17*(11), 1325–1329.

Howe, E. D. (1974), *Fundamentals of Water Desalination*, CRC Press, Boca Raton, Fla.

Hung, H.-M., Y. Katrib, and S. T. Martin (2005), Products and mechanisms of the reaction of oleic acid with ozone and nitrate radical, *J. Phys. Chem. A*, *109*(20), 4517–4530.

Katrib, Y., S. T. Martin, H.-M. Hung, Y. Rudich, H. Zhang, J. G. Slowik, P. Davidovits, J. T. Jayne, and D. R. Worsnop (2004), Products and mechanisms of ozone reactions with oleic acid for aerosol particles having core-shell morphologies, *J. Phys. Chem. A*, *108*(32), 6686–6695.

King, G. (1938), The oxidation of the 9:10-dihydroxystearic acids with periodic acid. η-Aldehydo-octoic acid., *J. Chem. Soc.*, 1826–1828.

Lu, R., W. Gan, B.-H. Wu, Z. Zhang, Y. Guo, and H.-F. Wang (2005), C–H stretching vibrations of methyl, methylene and methine groups at the vapor/alcohol (n = 1–8) interfaces, *J. Phys. Chem. B*, *109*(29), 14,118–14,129.

Ma, G., and H. C. Allen (2003), Surface studies of aqueous methanol solutions by vibrational broad bandwidth sum frequency generation spectroscopy, *J. Phys. Chem. B*, *107*(26), 6343–6349.

Ma, G., and H. C. Allen (2006), New insights into lung surfactant monolayers using vibrational sum frequency generation spectroscopy, *Photochem. Photobiol.* ASAP article 10.1562/2006-06-30-IR-958.

Mamane, H., J. J. Ducoste, and K. G. Linden (2006), Effect of particles on ultraviolet light penetration in natural and engineered systems, *Appl. Opt.*, *45*(8), 1844–1856.

McIntire, T. M., A. S. Lea, D. J. Gaspar, N. Jaitly, Y. Dubowski, Q. Li, and B. J. Finlayson-Pitts (2005), Unusual aggregates from the oxidation of alkene self-assembled monolayers: A previously unrecognized mechanism for SAM ozonolysis?, *Phys. Chem. Chem. Phys.*, *7*, 3605–3609.

Miranda, P. B., and Y. R. Shen (1999), Liquid interfaces: A study by sum-frequency vibrational spectroscopy, *J. Phys. Chem. B*, *103*(17), 3292–3307.

Mmereki, B. T., D. J. Donaldson, J. B. Gilman, T. L. Eliason, and V. Vaida (2004), Kinetics and products of the reaction of gas-phase ozone with anthracene adsorbed at the air-aqueous interface, *Atmos. Environ.*, *38*(36), 6091–6103.

Moise, T., and Y. Rudich (2002), Reactive uptake of ozone by aerosol-associated unsaturated fatty acids: Kinetics, mechanism, and products, *J. Phys. Chem. A*, *106*(27), 6469–6476.

Morris, J. W., P. Davidovits, J. T. Jayne, J. L. Jimenez, Q. Shi, C. E. Kolb, D. R. Worsnop, W. S. Barney, and G. Cass (2002), Kinetics of submicron oleic acid aerosols with ozone: A novel aerosol mass spectrometric technique, *Geophys. Res. Lett.*, *29*(9), 1357, doi:10.1029/2002GL014692.

Raja, S., and K. T. Valsaraj (2005), Heterogeneous oxidation by ozone of naphthalene adsorbed at the air–water interface of micron-size water droplets, *J. Air Waste Manage. Assoc.*, *55*(9), 1345–1355.

Richmond, G. L. (2002), Molecular bonding and interactions at aqueous surfaces as probed by vibrational sum frequency spectroscopy, *Chem. Rev.*, *102*(8), 2693–2724.

Rogge, W. F., L. M. Hildemann, M. A. Mazurek, G. R. Cass, and B. R. T. Simoneit (1991), Sources of fine organic aerosol. 1. Charbroilers and meat cooking operations, *Environ. Sci. Technol.*, *25*(6), 1112–1125.

Seeley, J. V., A. W. Bull, R. J. Fehir Jr., S. Cornwall, G. A. Knudsen, and S. K. Seeley (2005), A simple method for measuring ground-level ozone in the atmosphere, *J. Chem. Educ.*, *82*(2), 282–285.

Smith, G. D., E. Woods III, T. Baer, and R. E. Miller (2003), Aerosol uptake described by numerical solution of the diffusion-reaction equations in the particle, *J. Phys. Chem. A*, *107*(45), 9582–9587.

Socrates, G. (2001), *Infrared and Raman Characteristic Group Frequencies*, John Wiley, Hoboken, N. J.

Srisankar, E. V., and L. K. Patterson (1979), Reactions of ozone with fatty acid monolayers: A model system for disruption of lipid molecular assemblies by ozone, *Arch. Environ. Health*, *34*(5), 346–349.

Tervahattu, H., K. Hartonen, V.-M. Kerminen, K. Kupiainen, P. Aarnio, T. Koskentalo, A. F. Tuck, and V. Vaida (2002a), New evidence of an organic layer on marine aerosols, *J. Geophys. Res.*, *107*(D7), 4053, doi:10.1029/2000JD000282.

Tervahattu, H., J. Juhanoja, and K. Kupiainen (2002b), Identification of an organic coating on marine aerosol particles by TOF-SIMS, *J. Geophys. Res.*, *107*(D16), 4319, doi:10.1029/2001JD001403.

Tervahattu, H., J. Juhanoja, V. Vaida, A. F. Tuck, J. V. Niemi, K. Kupiainen, M. Kulmala, and H. Vehkamaki (2005), Fatty acids on continental sulfate aerosol particles, *J. Geophys. Res.*, *110*(D6), D11104, doi:10.1029/2004JD005408.

Thornberry, T., and J. P. D. Abbatt (2004), Heterogeneous reaction of ozone with liquid unsaturated fatty acids: Detailed kinetics and gas-phase product studies, *Phys. Chem. Chem. Phys.*, *6*(1), 84–93.

Vogel, V., C. S. Mullin, Y. R. Shen, and M. W. Kim (1991), Surface density of soluble surfactants at the air/water interface: Adsorption equilibrium studied by second harmonic generation, *J. Chem. Phys.*, *95*(6), 4620–4625.

Voss, L. F., C. M. Hadad, and H. C. Allen (2006), Replacement of atmospherically relevant fatty acid monolayers at the air/water interface, *J. Phys. Chem. B*, *110*(39), 19,487–19,490.

Wadia, Y., D. J. Tobias, R. Stafford, and B. J. Finlayson-Pitts (2000), Real-time monitoring of the kinetics and gas-phase products of the reaction of ozone with an unsaturated phospholipid at the air–water Interface, *Langmuir*, *16*(24), 9321–9330.

Yalkowsky, S. H., and Y. He (2003), *Handbook of Aqueous Solubility Data*, CRC Press, Boca Raton, Fla.

Zhang, D., J. Gutow, and K. B. Eisenthal (1994), Vibrational spectra, orientations, and phase transitions in long-chain amphiphiles at the air/water interface: Probing the head and tail groups by sum frequency generation, *J. Phys. Chem.*, *98*(51), 13,729–13,734.

H. C. Allen, M. F. Bazerbashi, C. P. Beekman, C. M. Hadad, and L. F. Voss, Department of Chemistry, The Ohio State University, 100 West 18th Avenue, Columbus, OH 43210, USA. (allen@chemistry.ohio-state.edu; hadad@chemistry.ohio-state.edu)